

Diblock Copolymers at a
Homopolymer–Homopolymer–Interface:
A Monte Carlo Simulation

A. Werner, F. Schmid, K. Binder
Johannes Gutenberg Universität Mainz
D–55099 Mainz
and
M. Müller
University of Washington
Department of physics, Box 351560
Seattle, Washington 98195

August 28, 2018

Abstract

The properties of diluted symmetric A - B diblock copolymers at the interface between A and B homopolymer phases are studied by means of Monte Carlo (MC) simulations of the bond fluctuation model. We calculate segment density profiles as well as orientational properties of segments, of A and B blocks, and of the whole chain. Our data support the picture of oriented “dumbbells”, which consist of mildly perturbed A and B Gaussian coils. The results are compared to a self consistent field theory (SCFT) for single copolymer chains at a homopolymer interface. We also discuss the number of interaction contacts between monomers, which provide a measure for the “active surface” of copolymers or homopolymers close to the interface.

1 Introduction

Blending of polymeric substances is a straightforward and inexpensive way of creating new materials with improved mechanical properties[1]. However, long polymers of different type A and B are often immiscible already at high temperatures, since the total energy of the (usually repulsive) relative interaction is proportional to the total number of monomers and cannot be balanced by the entropy of mixing, which is proportional to the number of polymers in the mixture[2, 3]. In order to overcome this problem, block copolymers containing both types of monomers can be used as effective compatibilizers[4, 5]. Being partly compatible with both the A and B rich phase, they tend to aggregate at interfaces, where they reduce the number of direct contacts between A and B homopolymers, thereby reducing the interfacial tension[6]. Consequently the total area of interfaces increases, and the immiscible components may get finely dispersed in the mixture. Furthermore, copolymers improve the mechanical properties of such interfaces: Due to entanglement between homopolymers and copolymers, they increase the adhesive attraction and the fracture toughness[7, 8, 9]. At high enough copolymer concentrations, additional copolymer rich phases emerge which may display a diversity of structures ordered on a mesoscopic scale[10, 11].

The simplest possible copolymers are diblocks, which consist of a block of A monomers connected to a block of B monomers. From a thermodynamic point of view, their effect on interfaces can be described as follows: Copolymers act as amphiphiles in the homopolymer mixture[12]. Increasing the copolymer concentration causes the interfacial tension to decrease monotonically, until this process is terminated by the formation of a third, copolymer rich phase,

e.g. an ordered lamellar phase or microemulsion. The amphiphilic strength of a copolymer, *i.e.*, the maximum reduction of the interfacial tension it can achieve, increases with the length of the A and B blocks relative to the size of the homopolymers. Mean field theories predict that the interfacial tension can be driven to zero for long copolymers, which implies that the copolymer rich lamellar phase evolves into the two-phase region via a continuous unbinding transition[13, 14]. Fluctuations push the transition to first order in real systems[15]. One can argue that the low interfacial tensions at the presence of copolymers result from the affinity of the system to such an unbinding transition[16].

This macroscopic discussion however does not shed light on the microscopic mechanisms, why and how copolymers work as compatibilizer or amphiphiles. In a simple microscopic picture, the A block of copolymers at interfaces preferably stick into the A -rich phase, the B block into the B -rich phase, and the molecules as a whole act as reinforcing rods[7]. The conformations of the copolymers determine the properties of the interface. A more detailed microscopic description of copolymer properties at interfaces has been developed by Leibler[17] and refined by Semenov[18]. The analysis is based on the assumption, that the junction points between A and B blocks are confined to a narrow region, which is much smaller than the width of the copolymer layer at the interface. The presence of copolymers at the interface gives rise to two free energy contributions: the entropy of mixing, divided into a translational term and a swelling term, and the elastic energy of stretching of the copolymer blocks. A scenario emerges which distinguishes between four different regimes: In the dilute regime, copolymers aggregate at the interface, but do not yet

overlap. The A and B blocks are described as weakly perturbed coils, and the free energy is dominated by the mixing energy. When the mean interchain distance gets of the order of the block radii of gyration, copolymers start to stretch and form a “wet brush”. At even higher copolymer concentrations, the “dry brush” regime is entered, where homopolymers do not penetrate into the interfacial region; A and B blocks have the conformation of stretched coils and the free energy is dominated by the elastic energy of stretching. Finally, in the saturated regime, the density of copolymers at the interface is close to one and the interfacial segregation of copolymers competes with the formation of micelles in the bulk[18].

Experimental studies of copolymers at homopolymer interfaces have been carried out by numerous groups, mostly using neutron reflectivity or forward recoil spectroscopy [19]-[25]. By deuterating individual parts of the homopolymers or the copolymers, the excess of copolymers at the interface can be measured as well as distributions of homopolymer segments, copolymer segments or even selected copolymer segments, like the junction point between A and B or the end segment[25, 26, 27]. These studies have provided detailed insight into the microscopic structure of such interfaces.

Simple Leibler type theories are already quite successful in reproducing many of the experimental results[18, 24]. In order to reach quantitative agreement, however, the Flory Huggins parameter χ has to be treated as adjustable, molecular weight dependent parameter. Less transparent, but more accurate mean field approaches are the self consistent field theories[28, 29] or the density functional theories[30, 31]. The self consistent field theory has first been applied to copolymer-homopolymer interfaces by Noolandi and Hong[32] and

adjusted to the case of a blend without solvent by Shull and Kramer[33, 34]. It has been shown to be quantitatively successful in predicting the correct copolymer excess at the interface, using a χ -parameter which is taken from independent bulk measurements[25]. The calculated width of the segment interface is somewhat too low, but the discrepancies can be understood quantitatively if broadening due to capillary waves is accounted for[22, 25]. Such a remarkable success of a mean field theory is characteristic for polymeric substances, in which high molecular weight polymers interact with a high number of other polymers[2, 35]. In addition to reproducing experimental data, the self consistent field theory also has the advantage of yielding further structural information, e.g. on chain conformations, monomer orientations etc.[36, 45], which may be hard to access experimentally. Unfortunately, the theory also has some serious drawbacks. In particular, the usual treatment of polymers as Gaussian random walks is questionable for chains of the minority component, e.g. A in the B rich phase, and generally on length scales smaller than the screening length of the excluded volume[45].

Computer simulations provide another way of obtaining additional information on the microscopic structure of interfaces. Simulations of inhomogeneous polymeric systems are computationally extremely demanding, and therefore rare. Minchau et al [37] and Fried and Binder[38, 39] have investigated the phase behavior of pure copolymer systems. Pan et al studied microphase structures in systems of short copolymers, which are swollen by a small amount (volume fraction 10 %) of longer homopolymers[40]. Wang and Mattice have studied the adsorption of self avoiding copolymers at a stationary, sharp interface, modelled by an external field with a sharp kink[41]. A similar study

has been performed for a random copolymer by Peng et al [42]. More detailed simulations have been presented by Cifra[43].

In this work, we present a study of copolymers at the interface between homopolymer phases, where both homopolymers and copolymers are treated in microscopic detail. Pure homopolymer interfaces in immiscible A/B blends have been analyzed previously[44] and compared to the predictions of a self consistent field theory[45]. Here, we consider the effect of adding a small number of symmetric diblock copolymers to such a “known” homopolymer interface. We restrict ourselves to the diluted case, where the copolymer coils do almost not overlap, and where the static structure of the interface is essentially that of a pure homopolymer interface. The results are compared to self consistent field theory calculations for a single copolymer in a homopolymer interface. Our paper is organized as follows: The next section describes the simulation model and method, and ends with a few comments on the self consistent field theory. The results are presented in section three. In particular, we discuss segment density profiles, chain and bond orientations, and profiles for the number of interacting contacts between monomers. We summarize and conclude in the last section.

2 The Bond Fluctuation Model

With the presently available computational resources, molecular modelling of the phase behavior in polymer blends in atomistic detail is far beyond feasibility. Fortunately, many important features of such systems are already apparent in coarse grained models[46], such as the bond fluctuation model on a cubic lattice[47]. The latter models polymers as chains of N effective monomers,

which occupy each a cube of 8 neighboring sites and are connected by bond vectors of length $2, \sqrt{5}, \sqrt{6}, 3,$ or $\sqrt{10}$ in units of the lattice spacing a_0 . One such cube represents a group of $n \approx 3 - 5$ chemical monomers. Hence a total chain length of 32, as has been used here, corresponds to a degree of polymerization of approx. 100-160 in a real polymer. At volume fraction $\phi = 0.5 a_0^{-3}$ or monomer density $\rho = 1/16 a_0^{-3}$, the model reproduces many important properties of dense polymer melts, e.g. single chain configurations show almost ideal Gaussian chain statistics, the single chain structure factor follows a Debye function, and the collective scattering function has the experimental form[48].

The relative repulsion between monomers of type A and B is modelled by introducing symmetric energy parameters $\varepsilon_{AA} = \varepsilon_{BB} = -\varepsilon_{AB} = -k_B T \varepsilon$, which describe the pairwise interaction between monomers at distances of less than $\sqrt{6} a_0$. At $\varepsilon = 0.1$, the interactions between monomers are dominated by the effect of excluded volume, and the mixture can be described as a weakly perturbed athermal melt; in particular, the equation of state and the compressibility are almost not affected by the presence of the interactions[49]. From extensive previous study of this model, the relation of these model parameters to commonly used parameters in polymer theories is well known. At chain length $N = 32$, the statistical segment length b is given by $b = 3.05 a_0$ [44], the radius of gyration is $R_g = \sqrt{N/6} b \approx 7 a_0$, the compressibility is $k_B T \kappa = 3.9 a_0^3$ [49], and the Flory Huggins parameter χ can be calculated using $\chi = 2z\varepsilon$, where $z = 2.65$ is the effective coordination number in the bulk, *i.e.*, the average number of *interchain* contacts of a monomer[50].

The interfacial properties were studied in a $L \times D \times L$ geometry at system size $D = 64$ and $L = 512$. The dimensions of the system were chosen such

that the width D of the slab is much larger than the gyration radius R_g , *i.e.*, almost ten times as large. The boundary conditions are periodic in x and z direction and “antiperiodic” in the y direction, *i.e.*, A -chain parts leaving the right part of the simulation box reenter it on the left side as B -chain parts and vice versa. Since no mechanism fixes the interface at a certain position, the interface position is subject to diffusion due to thermal fluctuations. We choose the coordinate system such that the origin of the y -axis is at the center y_0 of the interfacial profile, which we determine via[51]

$$\left| \sum_{y_0-20}^{y_0+20} m(y) \right| = \min. \quad (1)$$

Here $m = \rho_A - \rho_B$ is the order parameter of the demixing transition and the relative monomer densities are defined by $\rho_{A,B} = \phi_{A,B}/\phi$, where ϕ_A and ϕ_B are the volume fractions taken by A and B monomers. The simulation box contains 32768 polymers of equal chain length 32. As initial configuration, we choose a relaxed configuration of a pure homopolymer interface[44], randomly pick 1024 chains with the center of mass at distances of less than $\pm\delta$ from the interface with $\delta = 3$ or 9, and turn them into copolymers. No effect of the choice of δ on the results has been found. The simulation algorithm involves random hopping of randomly chosen monomers by one lattice unit with Metropolis probability, but no grandcanonical moves, *i.e.*, the number of copolymers remains fixed. After an initial equilibration time of $2.5 \cdot 10^5$ attempted moves per monomer (AMM), the concentration of copolymers in the bulk at $\varepsilon = 0.1$ is $0.05\% \pm 0.01\%$ – estimates from grand canonical bulk simulations suggest that it should be around 0.04% [52]. We average over 86 configurations in total, where the data for averaging are taken every 10^4 AMM. The area covered by one copolymer can be roughly estimated by $\pi R_{g,b}^2$, where

$R_{g,b}^2 = b^2 N/12$ is the gyration radius of one copolymer block. Hence 1024 copolymers cover approximately 30% of the total interface area 512×512 , *i.e.*, the system is well in the diluted regime.

We close this section with a brief comment on the self consistent field calculations. In a previous paper, we have compared the properties of homopolymer interfaces with the predictions of self consistent field theories for completely flexible and semiflexible chains with different chain rigidities[45]. The qualitative agreement between theory and simulation was over all very good. The main quantitative discrepancy was found in the interfacial width – at chain length 32, the self consistent field theory underestimates the profile widths by at least a factor of 2. This effect could not be explained by capillary waves alone, but seemed to be a consequence of the short chain length. At temperatures sufficiently below the critical point, so that critical fluctuations do not affect the interface any more, the interfacial width gets already comparable to the screening length of the excluded volume, on which length scale chains can not be treated as pure random walks. This leads to wrong predictions of the size of the interface. However, theory and simulations still agree quantitatively for other quantities, e.g. the reduction of the total density at the interface.

Our present calculations are based on this work. We consider single wormlike copolymer chains at an interface of wormlike homopolymers. Chains are represented by space curves $\vec{r}(s)$ with s varying from 0 to 1, and the single chain partition function of a copolymer is given by

$$\mathcal{Z} = \int \widehat{\mathcal{D}}\{\vec{r}(\cdot)\} \exp \left[- \int_0^{1/2} ds W_A(\vec{r}(s)) - \int_{1/2}^1 ds W_B(\vec{r}(s)) \right], \quad (2)$$

where $W_i(\vec{r})$ is the self consistent field acting on a monomer of type i in a homopolymer interface. Each space curve is assigned a statistical weight in

the functional integral, $\widehat{\mathcal{D}}\{\vec{r}(\cdot)\} = \mathcal{D}\{\vec{r}(\cdot)\}\mathcal{P}_W\{\vec{r}(\cdot)\}$ with[53]

$$\mathcal{P}_W\{\vec{r}(\cdot)\} = \mathcal{N} \prod_s \delta(\vec{u}^2 - 1) \exp\left[-\frac{\eta}{2N} \int_0^1 ds \left|\frac{d\vec{u}}{ds}\right|^2\right], \quad (3)$$

where a is the fixed monomer length, η a dimensionless stiffness parameter, $\vec{u} = \frac{d\vec{r}}{ds}/(Na)$ the dimensionless tangent vector constrained to unity by the delta function, and \mathcal{N} the normalization factor. Here we choose $\eta = 0.5$, the value which best reproduces bond orientations in pure homopolymer interfaces in the bond fluctuation model[45]. The self consistent fields W_i for such an interface of semiflexible homopolymers have previously been determined numerically in Ref. [45], based on the Helfand type free energy functional

$$\beta\mathcal{F} = \rho \int d\vec{r} \left\{ \chi \Phi_A \Phi_B + \frac{1}{2\rho k_B T \kappa} (\Phi_A + \Phi_B - 1)^2 \right\} \quad (4)$$

with the total bulk monomer density ρ , the relative monomer densities $\Phi_i(\vec{r}) = \rho_i(\vec{r})/\rho$ ($i = A$ or B), the Flory Huggins parameter χ , and the compressibility κ .

The distribution of copolymer segments is calculated by solving appropriate diffusion equations for the end segment distributions $Q(\vec{r}, \vec{u}; s)$ and $Q^+(\vec{r}, \vec{u}; s)$ for chain parts of length $sN < N$, which begin on the A side (Q) or the B side (Q^+) of the copolymer[54, 55]. From those one can calculate the density of monomers at position s with orientation \vec{u} via $\Phi(\vec{r}, s) = Q(\vec{r}, s)Q^+(\vec{r}, 1 - s)$ or $\Phi(\vec{r}, \vec{u}) = Q(\vec{r}, \vec{u}, s)Q^+(\vec{r}, -\vec{u}, 1 - s)$. The numerical treatment is facilitated by expanding the functions Q, Q^+ in Legendre polynomials and including only the three lowest moments[45].

3 Results

All results presented here were obtained at $\varepsilon = 0.1$ or $\chi N = 17$, *i.e.*, the system is far from the critical point ($(\chi N)_c = 2.4$ [48, 50]) in the strong segregation regime. Simulations were also performed at $\varepsilon = 0.05$; the results are qualitatively the same, but the effects are less marked.

In the following, lengths are given in units of $w_{SSL} = b/\sqrt{6\chi}$, the interfacial width of a homopolymer interface in the mean field strong segregation limit. The radius of gyration in these units is $R_g = 4.2 w_{SSL}$, and the slab thickness $D = 37.4 w_{SSL}$.

3.1 Density profiles and segment distributions

Figure 1 shows profiles of A and B monomer densities in systems with and without copolymers, profiles of just the A and B blocks of the copolymers, and total density profiles. As expected in the diluted regime, the A and B monomer density profiles are hardly affected by the presence of the copolymers. The interface as a whole is still very similar to a pure homopolymer interface. Due to the finite compressibility of the blend, the total density is slightly reduced in the interfacial region[44]. The distributions of copolymer monomers A and B agree qualitatively with the experimental results and confirm the simple picture presented in the introduction: Monomers of type A are more concentrated in the A -rich phase, Monomers of type B in the B rich-phase. The distribution is rather broad, a fair portion of the A monomers sticks into the B -rich phase and vice versa.

Distributions of single chain segments are shown in Figure 2 and 3. For homopolymers, one finds a relative enrichment of chain ends ρ_e at the inter-

face, whereas the concentration $\rho_{1/2}$ of middle segments (the 16th and 17th monomer) is comparatively low there. The total density profile ρ_h is best reproduced by the density profiles $\rho_{1/4}$ of the segments at one and three fourth of the chain (the 8th and 25th monomer). Looking at the higher concentration of chain ends at the interface, one is lead to suspect that homopolymers tend to form loops with two ends at the interface. However, this is not the case, as can be seen from the distribution ρ_{e-e} of midpoints between the two ends of homopolymers. It is strongly reduced at the center of the interface and enhanced at the distance of one gyration radius from there (Figure 2).

Copolymer segment densities show the inverse trend: The middle segments concentrate at the interface, whereas the chain ends stretch out into their favorite bulk phase. Hence our results are in qualitative agreement with the experimental findings of Russell et al [25]. As in the case of homopolymers, the total density profiles of A and B monomers are almost identical with the distribution of the 8th and 25th monomer, respectively, *i.e.*, the distribution of segments in the middle of the A or B block. Note that the peak of the distribution of middle segments $\rho_{1/2}$ is relatively broad, broader than the radius of gyration, hence they are not strongly confined to the interface as assumed by the Leibler theory (Figure 3). The results of the self consistent field theory are shown in the inset. The fact that the SCFT underestimates the interfacial width also leads to quantitative discrepancies in the distribution of copolymer segments. However, the qualitative agreement is very good, and in the wings of the profile one even reaches quantitative agreement.

3.2 Chain and bond orientations

Next we discuss the orientational properties of the polymers. It is instructive to consider separately the orientations of single bonds, of chain segments, and of whole chains. Chains with rather weakly oriented single bonds can still be strongly oriented as a whole, as found by Müller et al for homopolymers at a homopolymer interface[44, 45].

The orientation of whole chains involves two different factors. First, chains may be oriented without volume changes, *i.e.*, the total gyration radius or end-to-end vector remains unaffected by the orientation. A weak orienting field is sufficient to bring about orientation of this kind. Second, chains may get compressed or stretched in one direction. As Figure 4 illustrates, the latter effect dominates close to an interface. The mean squared components of the end-to-end vector in directions parallel (x,z) and perpendicular (y) to the interface are shown for homopolymers and copolymers. The components parallel to the interface hardly vary throughout the system. Perpendicular to the interface, the end-to-end vector of homopolymers is reduced in the interfacial region, as is already the case in pure homopolymer systems. Homopolymers are thus squeezed perpendicular to the interface, and get effectively oriented parallel to the interface.

Copolymers show the inverse behavior, they stretch in the direction perpendicular to the interface. As obtained both from self consistent field calculations and from the simulations, the effect is very strong for copolymers centered at about one to two radii of gyration away from the interface, and much weaker for those located in the wings of profile or at the middle of the interface (Figure 4). One can picture the latter as consisting of two almost independent

homopolymer blocks, which hardly feel the effect of being linked together at one end. Indeed, the vector connecting the ends of the single A or B blocks is on average hardly oriented (Table 1). Only the blocks centered deep in their majority phase ($y/w_{SSL} \approx 7$) stretch perpendicular to the interface, since they are pulled towards the interface by the other copolymer end (Figure 5). Note that Figure 5 also demonstrates, how minority blocks (A blocks in the B phase, B blocks in the A phase) slightly shrink by a factor of approximately 0.8 due to the hostile environment. The vector \vec{D}_{AB} connecting the centers of mass of the A and B blocks is on average oriented and strongly stretched in the negative y direction (Table 1).

In sum, single blocks are mostly not oriented at all; the perpendicular orientation of whole copolymers results from the arrangement of the two constituent blocks. Diblock copolymers can be pictured as dumbbells[56] consisting of two mildly perturbed homopolymer coils. Similar copolymer shapes have already been found by Binder and Fried in simulations of block copolymers in the disordered phase, far above the ordering transition[39].

Consequently, one would expect that the only region, where the local conformation of a diblock differs significantly from a homopolymer conformation, is the region close to the link which connects the two blocks. We study this in more detail by looking at the orientation of single bonds \vec{b} . In order to do so, it is useful to define a bond orientation parameter

$$q(\vec{r}) = \frac{\langle b_y^2 \rangle - \frac{1}{2}(\langle b_x^2 \rangle + \langle b_z^2 \rangle)}{\langle b^2 \rangle}. \quad (5)$$

Negative q implies orientation parallel to the interface, positive q perpendicular orientation.

The orientations of homopolymer bonds are shown in Figure 6. Like whole

chains, but to a much lesser extent, bonds tend to align themselves parallel to the interface. Unlike the end-to-end vector of whole chains, the average squared bond length $\langle \vec{b}^2 \rangle$ varies by less than 0.15% throughout the system (not shown here), hence the bond length is quasi fixed, the bonds get oriented without compression. The effect is strongest in the middle of the chains and qualitatively the same, but weaker for end bonds. The bond orientation parameter can be compared to the average orientation of the tangent vector \vec{u} predicted by the self consistent field theory $q \hat{=} \frac{1}{2}(3\langle u_y^2 \rangle - 1)$. The results show the same trend as the simulation data for the middle bonds, but do not predict any effect for the end bonds (Figure 6, inset), unlike what is seen in the MC simulations. This reflects the difference between the tangent vector at the end of a continuous space curve, as assumed by SCFT, and an end bond connecting two discrete statistical monomers of a relatively short chain, as it is the case in our MC simulation.

In contrast to homopolymer chains, MC data reveal a rather strong dependence of the orientation of bonds in copolymers on their position within the chain (Figure 7a). The bond which links the two blocks is preferably oriented perpendicular to the interface – the stronger, the further away its location from the center of the interface. Already the bonds next to the link bond show a much smaller effect. The larger the distance along the chain from the link bond, the stronger the tendency of parallel alignment at the center of the interface becomes, and the further it reaches out into the wings of the profile. Hence bonds in the middle and at the end of an A or B block behave very much like homopolymer bonds. We note *en passant* that, compared to the other bonds, the link bond is stretched by $\sim 4\%$ due to the relative repulsion

between the adjacent A and B monomers.

The results obtained by SCFT show the same trends as the simulation data (Figure 7b), and agree qualitatively, but the same remarks as above apply. Thus, SCFT does not reproduce the slight tendency of parallel alignment which is found in the MC data at the ends of the blocks. The orientational parameter of the link bond at the center of the profile is $q \approx +0.025$ according to both MC results and SCFT. However, SCFT underestimates the average orientation (averaged over link bonds in the region shown in Figure 7a) by $\sim 30\%$. At distances of several gyration radii R_g from the interface, the bond orientation parameter q drops back to zero, indicating that copolymers that deep in the bulk are oblivious to the effect of the interface. Note that two different length scales are reflected in the profiles of q . One of them, the width of the homopolymer interface, fixes the width of the central dip in the profiles, the other one, the gyration radius, determines the overall width of the region with nonzero q .

3.3 Self and Mutual Contacts

Another instructive quantity in the bond fluctuation model is the number of monomer “contacts”, *i.e.*, the number of interacting monomer pairs. It is expedient to distinguish between “self contacts”, *i.e.*, contacts between monomers belonging to the same chain (“intrachain contacts”), and “interchain contacts” of monomers from two different chains. The self contacts provide additional information on the conformation of single chains, and the interchain contacts on the arrangement of chains relative to each other.

Figure 8 compares the number of self contacts per monomer $N_{i,self}/\rho_i$ in

homopolymer ($i = h$) and copolymer ($i = c$) chains. The main contribution to $N_{i,self}/\rho_i$ comes from the two direct neighbors of a monomer in the chain, thus $N_{i,self}/\rho_i$ is mostly slightly larger than 2. Note however that direct neighbors do not always interact with each other, since the maximum bond length $\sqrt{10}a_0$ is larger than the range of the interactions $\sqrt{6}a_0$. The number of self contacts in homopolymers is almost constant throughout the system. It is slightly enhanced in the wings of the profile and decreases again at the center, where A and B meet – suggesting that homopolymer chains tend to loop away from the interface, such that there is no room for intrachain contacts at the center, but that the number of contacts increases right next to it. In copolymers, one finds the opposite behavior – the relative number of intrachain contacts is higher at the center of the interface than in homopolymers, but diminishes rapidly as one moves away from the interface. This trend is promoted by three factors. First, far from the interface copolymers stretch towards the interface, and the number of self contacts associated with backfolding goes down. Second, the stretching goes along with a higher occupation of the $(0, 3, 0)$ bond, which is outside of the interaction region, hence monomers gradually lose contact to their direct neighbors. Third, the further away one moves from the interface, the greater becomes the contribution of chain end monomers, which only have one direct neighbor in the chain. Obviously, it would be highly desirable to study separately the contributions to $N_{i,self}/\rho_i$ from monomers which are direct neighbors in a chain, and from monomers which are further apart from each other. Unfortunately, such a distinction was not possible due to limited memory space.

Whereas the number of self contacts reflects the conformational properties

of a chain, the demixing of A and B chains in the melt is essentially driven by the interchain contacts. The number of interchain contacts per monomer can be interpreted as an effective coordination number z_{eff} . In homogeneous systems, the identification $\chi = 2z_{eff}\varepsilon$ makes contact with the Flory-Huggins theory[50]. In inhomogeneous systems, the effective coordination number is position dependent. As long as the finite range of interactions is neglected, mean field theory simply asserts that it is proportional to the local density of monomers:

$$z_{i,eff}(\vec{r}) = \frac{N_{i,inter}(\vec{r})}{\rho_i(\vec{r})} \propto \rho(\vec{r}) \quad (6)$$

A more elaborated mean field approach predicts for a system which is inhomogeneous in one direction y [57],

$$z_{eff} \propto \rho(y) + \frac{1}{2}k^2 \frac{d^2}{dy^2}\rho(y) \quad \text{with} \quad k^2 = \frac{\int d\vec{r}\gamma(\vec{r})V(\vec{r})y^2}{\int d\vec{r}\gamma(\vec{r})V(\vec{r})}, \quad (7)$$

where $V(\vec{r})$ is the integrable part of the interaction potential (*i.e.*, excluding the hard core part) and $\gamma(\vec{r})$ the normalized pair correlation function. Since the interaction region extends no further than $|y| \leq 2a_0$, an upper bound for the factor k^2 is given by $k^2 \leq 4a_0^2$. Figure 1 shows that $\rho''(y)/\rho(y) \leq 0.01/a_0^2$. Hence the expected deviation from the simple proportionality law (6) is of order $\leq 2\%$. Furthermore, one would expect that the effective coordination number does not depend on whether a monomer belongs to a copolymer or a homopolymer.

In contrast to these considerations, the Monte Carlo data reveal a much lower dip of the reduced coordination number $z_{eff}(y)/\rho(y)$ (Figure 9) at the center of the interface. The discrepancy between mean field assumption and simulation data becomes even more manifest when looking at the number

of contacts N_{AB} between A and B monomers. From the usual mean field assumption, one would expect $N_{AB} \propto \rho_A \cdot \rho_B$ (Figure 10). The simulation data however show that $N_{AB}/(\rho_A\rho_B)$ is increased by a factor of 1.5, compared to the bulk value, at the distance of approximately two radii of gyration from the interface, where the chains are stretched (cf. Figure 5). At the center of the interface, on the other hand, it is decreased by 25%.

One can deduce that chains are compactified in the interfacial region. Interestingly, this holds particularly for copolymer chains. We recall that the number of *intrachain* contacts in copolymers is enhanced at the interface, whereas the *interchain* contacts are obviously suppressed. Thus copolymers offer relatively little “active surface” for interaction with external monomers in the interfacial region. In contrast, the relative number of external contacts increases further away from the interface. Hence the active surface per monomer will presumably increase with the copolymer chain length. This may be an additional reason why short copolymers are relatively poor amphiphiles.

3.4 Summary

We have studied the ternary system of A and B homopolymers and symmetric AB diblock copolymers close to an A/B interface in the dilute regime, where copolymer coils do almost not overlap with each other, by Monte Carlo simulations of the bond fluctuation model. In this regime, the structural properties of the interface are not altered with respect to the pure homopolymer interface – in particular, we find no significant broadening of the interfacial width, as is expected at higher copolymer concentrations. According to our simulation results, copolymers resemble oriented dumbbells with the A block

sticking into the A rich phase, and the B block sticking into the B rich phase. The conformations of single blocks are not very different from conformations of pure homopolymer coils. Single blocks tend to orient themselves parallel to the interface, like homopolymers, whereas copolymers as a whole are oriented perpendicular to the interface. When looking at the orientations of single bonds, we find that the orientational properties of the central bond, which links the two blocks, differ distinctly from those of a homopolymer bond, but that already the neighboring bonds behave very similar to homopolymer bonds. Hence the chain loses the memory of the link very rapidly. Our results are reproduced qualitatively, but not quantitatively, by a self consistent field calculation. Furthermore, we found that copolymers are unusually compact in the interfacial region, *i.e.*, monomers have more contacts to monomers of the same chain, and fewer contacts to monomers of different chains than monomers in the bulk phase. As a result, the copolymer-copolymer interchain contacts are particularly suppressed at the interface. This should become important as the concentration of copolymers is increased. Future work will be concerned with the structure of interfaces with higher content of copolymers and with the transition between different regimes, from the dilute to the wet brush to the dry brush regime, until the two phase region breaks down and a lamellar phase emerges.

Acknowledgements

We thank H. Weber for invaluable help in solving some computational problems. K.B. thanks W.L. Mattice for stimulating discussions. A.W. received partial support from the Deutsche Forschungsgemeinschaft under grant No. Bi

314/3-4. Further support from grant No. Bi 314/12-1, and generous access to the Cray T3D at EPFL is acknowledged.

References

- [1] see, for example, Paul, D.R.; Newman, S. *Polymer Blends*; Academic Press: New York, 1978; Šolc, K. (Ed.) *Polymer Compatibility and Incompatibility – Principles and Practices*; Harwood: Chur, 1982; Walsh, D.S.; Higgins, J.S.; Maconnachie, A. *Polymer Blends and Mixtures*; Martinus Nijhoff: Dordrecht, 1985; Thomas, E.L. (Ed.) *Materials Science and Technology, Vol. 12: Structure and Properties of Polymers*; VCH: Weinheim, 1993.
- [2] De Gennes, P.-G. *Scaling Concepts in Polymer Physics*; Cornell University Press: Ithaca, NY, 1979.
- [3] Sanchez, I.C. (Ed.) *Physics of Polymer Surfaces and Interfaces*; Butterworth–Heinemann: Boston, 1992; Fleer, G.J.; Cohen Stuart, M.A.; Scheutjens, J.M.H.M.; Cosgrove, T.; Vincent, B. *Polymers at Interfaces*; Chapman & Hall: London, 1993.
- [4] Bates, F.S.; Fredrickson, G.H. *Annu. Rev. Phys. Chem.* **1990**, *41*, 525; *Ann. Rev. Mater. Sci.*, submitted.
- [5] Binder, K. *Advances in Polymer Science* **1994**, *112*, 181.
- [6] Anastasiadis, S.H.; Gancarz, I.; Koberstein, J.T. *Macromolecules* **1989**, *22*, 1449.

- [7] Brown, H.R. *Macromolecules* **1989**, *22*, 2859; Brown, H.R.; Deline, V.R.; Green, P.F. *Nature* **1989**, *341*, 221; Brown, H.R.; Char, K.; Deline, V.R.; Green, P.F. *Macromolecules* **1993**, *26*, 4155.
- [8] Dai, C.A. *et al Phys. Rev. Lett.* **1994**, *73*, 2472.
- [9] Lee, Y.; Char, K. *Macromolecules* **1994**, *27*, 2603.
- [10] Kinning, D.J.; Winey, K.I.; Thomas, E.L. *Macromolecules* **1988**, *21*, 3502; Kinning, D.J. *et al J. Chem. Phys.* **1989**, *90*, 5806; Winey, K.I.; Thomas, E.L.; Fetters, L.J. *J. Chem. Phys.* **1991**, 9367; *Macromolecules* **1992**, *25*, 422; Hashimoto, T. *et al Macromolecules* **1993**, *25*, 1433; Disko, M.M. *et al Macromolecules* **1993**, *26*, 2983.
- [11] Leibler, L.; Pincus, P.A. *Macromolecules* **1984**, *17*, 2922; Semenov, A.N. *Macromolecules* **1993**, *26*, 2273.
- [12] Holyst, R.; Schick, M. *J. Chem. Phys.* **1992**, *96*, 7728.
- [13] Matsen, M.W. *Phys. Rev. Lett.* **1995**, *74*, 4225; *Macromolecules* **1995**, *28*, 5765.
- [14] Israels, R. *et al J. Chem. Phys.* **1995**, *102*, 8149.
- [15] Bates, F.S. *et al Phys. Rev. Lett.* **1995**, *75*, 4429.
- [16] Schick, M. *Ber. d. Bunsenges.*, in press.
- [17] Leibler, L. *Makromol. Chem., Macromol. Symp.* **1988**, *16*, 1.
- [18] Semenov, A.N. *Macromolecules* **1992**, *25*, 4967.
- [19] Löwenhaupt, B.; Hellmann, G.P. *Colloid Polym. Sci.* **1990**, *268*, 885.

- [20] Bucknall, D.G.; Higgins, J.S.; Penfold, J. *Physica B* **1992**, *180 & 181*, 468.
- [21] Shull, K.R.; Kramer, E.J.; Hadziioannou, T.; Tang, W. *Macromolecules* **1990**, *23*, 4780.
- [22] Dai, K.H.; Norton, L.J.; Kramer, E.J. *Macromolecules* **1994**, *27*, 1949;
Dai, K.H.; Washiyama, J.; Kramer, E.J. *Macromolecules* **1994**, *27*, 4544.
- [23] Russell, T.P. *et al Macromolecules* **1991**, *24*, 1575.
- [24] Green, P.F.; Russell, T.P. *Macromolecules* **1991**, *24*, 2931.
- [25] Shull, K.R.; Mayes, A.M.; Russell, T.P. *Macromolecules* **1993**, *26*, 3929.
- [26] Mayes, A.M.; Russell, T.P.; Satija, S.K.; Majkrzak, C.F. *Macromolecules* **1992**, *25*, 6523.
- [27] Mayes A.M. *et al Macromolecules* **1993**, *26*, 1047.
- [28] Helfand, E.; Tagami, Y. *J. Polym. Sci. B* **1971**, *9*, 741; *J. Chem. Phys.* **1971**, *56*, 3592; **1972**, *57*, 1812; Helfand, E.; Sapse, A.M. *J. Chem. Phys.* **1975**, *62*, 1327.
- [29] Helfand, E. *J. Chem. Phys.* **1975**, *62*, 999.
- [30] Tang, H.; Freed, K.F. *J. Chem. Phys.* **1991**, *94*, 6307; Dudowicz, J; Freed K.F. *Macromolecules* **1990**, *23*, 1519; Lifschitz, M.; Freed, K.F. *J. Chem. Phys.* **1993**, *98*, 8994.
- [31] Freed, K.F. *J. Chem. Phys.* **1995**, *103*, 3230.
- [32] Noolandi, J.; Hong, K.M. *Macromolecules* **1982**, *15*, 482; **1984**, *17*, 1531.

- [33] Shull, K.R.; Kramer, E.J. *Macromolecules* **1990**, *23*, 4769.
- [34] Shull, K.R. *Macromolecules* **1993**, *26*, 2346.
- [35] Binder, K. *J. Chem. Phys.* **1983**, *79*, 6387; *Phys. Rev. A* **1984**, *29*, 341.
- [36] Fischel, L.B.; Theodorou, D.N. *Faraday Trans.* **1995**, *91*, 2381.
- [37] Minchau, B.; Dünweg, B.; Binder, K. *Pol. Comm.* **1990**, *31*, 348.
- [38] Fried, H.; Binder, K. *J. Chem. Phys.* **1991**, *94*, 8349; *Europhys. Lett.* **1991**, *16*, 237.
- [39] Binder, K.; Fried, H. *Macromolecules* **1993**, *26*, 6878.
- [40] Pan, H. *et al Macromolecules* **1993**, *26*, 2860.
- [41] Wang, Y.; Mattice, W.L. *J. Chem. Phys.* **1993**, *98*, 9881; Wang, Y.; Li, Y.; Mattice, W.L. *J. Chem. Phys.* **1993**, *99*, 4068.
- [42] Peng, G.; Sommer, J.-U.; Blumen, A., preprint.
- [43] Cifra, P., Poster presented on the *International Workshop on Wetting and Self-Organization in Thin Liquid Films*, Konstanz, September 1995.
- [44] Müller, M.; Binder, K.; Oed, W. *J. Chem. Soc. Faraday Trans.* **1995**, *91*, 2369.
- [45] Schmid, F.; Müller, M. *Macromolecules* **1995**, *28*, 8639.
- [46] Binder, K. (Ed.) *Monte Carlo and Molecular Dynamics Simulations in Polymer Science*; Oxford University Press: Oxford, 1995.
- [47] Carmesin, I.; Kremer, K. *Macromolecules* **1988**, *21*, 2819.

- [48] Paul, W.; Binder, K.; Heermann, D.W.; Kremer, K. *J. Phys. II (Paris)* **1991**, *1*, 37; Deutsch, H.-P.; Binder, K. *Macromolecules* **1992**, *25*, 6214; *J. Phys. II (Paris)* **1993**, *3*, 1049.
- [49] Müller, M.; Paul, W. *J. Chem. Phys.* **1993**, *100*, 719.
- [50] Müller, M.; Binder, K. *Macromolecules* **1995**, *28*, 1825.
- [51] Schmid, F.; Binder, K. *Phys. Rev. B* **1992**, *46*, 13553.
- [52] Müller, M.; Schick, M.; document in preparation.
- [53] Kratki, O.; Porod, G. *Rec. Trav. Chim.* **1949**, *68*, 1106; Saito, N; Takahashi, K.; Yunoki, Y. *J. Phys. Soc. Jpn.* **1967**, *22*, 219.
- [54] Morse, D.C.; Fredrickson, G.H. *Phys. Rev. Lett.* **1994**, *73*, 3235.
- [55] Matsen, M.W.; Schick, M. *Phys. Rev. Lett.* **1994**, *72*, 2660; Matsen, M.W. *J. Chem. Phys.*, **1996**, *104*, 7758.
- [56] Weyersberg, A.; Vilgis, T.A. *Phys. Rev. E* **1993**, *48*, 377.
- [57] Schmid, F., *J. Chem. Phys.*, **1996**, *104*, 9191.

Table

Table 1: Orientational properties of copolymer chains. Averages are taken over all 1024 copolymers and over 86 independent configurations. Compared are x, z components (together) with y components. Lengths are given in units of w_{SSL} .

		$i = x, z$	$i = y$
end-to-end vector: A and B blocks ($N = 16$)	$\langle R_i^2 \rangle$	15.3	15.6
whole copolymer chain ($N = 32$)	$\langle R_i^2 \rangle$	32.7	47.4
vector from center of block A to center of block B	$\langle D_{i,AB}^2 \rangle$	11.6	19.4
	$\langle D_{i,AB} \rangle$	0.0	-3.8

Figure Captions

Figure 1: Monomer density profiles as a function of the distance from the center of the interface y , in units of $w_{SSL} = b/\sqrt{6\chi} = 1.71 a_0$. Profiles are shown for the density of all monomers (ρ), of A and B monomers separately (ρ_A and ρ_B), of just homopolymer monomers (ρ_h), and of A and B monomers belonging to a copolymer block ($\rho_{A,c}$ and $\rho_{B,c}$). Also shown for comparison are A and B monomer profiles in a pure homopolymer system (ρ_A^0 and ρ_B^0 , taken from [44]).

Figure 2: Homopolymer segment density profiles vs. y/w_{SSL} in units of $w_{SSL} = b/\sqrt{6\chi}$. Profiles are shown for the density of monomers in the middle of the chain ($\rho_{1/2}$), at the end of the chain (ρ_e), at one and three fourth of the chain ($\rho_{1/4}$), and of all homopolymer monomers (ρ_h). Also shown is the distribution of midpoints between the two ends of homopolymers, ρ_{e-e} . Units of densities are the total bulk concentration of monomers ρ_b , or $\rho_{sb} = \rho_b/16$ (as indicated).

Figure 3: Copolymer segment density profiles vs. y/w_{SSL} in units of $w_{SSL} = b/\sqrt{6\chi} = 1.71 a_0$. Profiles are shown for the density of A and B monomers in the middle of the chain ($\rho_{1/2}$, squares), at the end of the chain (ρ_e , circles), at one and three fourth of the chain ($\rho_{1/4}$, diamonds), and of all copolymer monomers (ρ_c , broken line). Inset shows results of the self consistent field theory for A monomers. Full lines show the predictions for segment density profiles $\rho_{1/2}$, ρ_e , $\rho_{1/4}$, broken line shows total density profile ρ_c , and symbols compare with MC results (symbols like above). Units of densities are $\rho_b/2$, or $\rho_{sb} = \rho_b/32$ (as indicated).

Figure 4: Mean square end-to-end vector components $\langle R_i^2 \rangle$ with $i = x, y, z$ in units of the average bulk value $b^2 N/3$, plotted vs. the distance of the center of the end-to-end vector from the interface y in units of $w_{SSL} = b/\sqrt{6\chi}$. Results are shown for homopolymers and copolymers, and compared to the prediction for copolymers of the self consistent field theory.

Figure 5: Mean square end-to-end vector components $\langle R_i^2 \rangle$ ($i = x, z$, or y) of the copolymer blocks in their minority phase (A block in B phase, B block in A phase), and majority phase (A block in A phase, B in B phase), in units of the average bulk value $b^2 N/6$, plotted vs. the distance of the center of the end-to-end vector from the interface y in units of $w_{SSL} = b/\sqrt{6\chi}$.

Figure 6: Orientational order parameter q for end bonds (dashed line) and middle bonds (the bonds connecting the 16th and 17th monomer, solid line) in homopolymers, vs. y/w_{SSL} in units of $w_{SSL} = b/\sqrt{6\chi}$. Inset shows the prediction of the self consistent field theory.

Figure 7: (a) Orientational order parameter q for end bonds, link bonds (linking 16th and 17th monomer), bonds next to link bonds (15th to 16th monomer and 17th to 18th monomer), and bonds in the middle of a block (8th to 9th monomer and 24th to 25th monomer) in copolymers, vs. y/w_{SSL} in units of $w_{SSL} = b/\sqrt{6\chi}$. (b) Prediction for q of the self consistent field theory for $s = (0, 1)$ (end bonds), $s = 0.5$ (link bonds), $s = (0.25, 0.75)$ (block middle bonds).

Figure 8: Number of intrachain contacts per monomer $N_{i,self}/\rho_i(y)$ ($i = h, c$) vs. y/w_{SSL} in units of $w_{SSL} = b/\sqrt{6\chi}$ for homopolymer and copolymer

chains.

Figure 9: Normalized effective coordination number $z_{eff}(y)/\rho(y)$ vs. y/w_{SSL} in units of $w_{SSL} = b/\sqrt{6\chi}$, for homopolymer and copolymer chains.

Figure 10: Normalized number of AB contacts $N_{AB}/(\rho_A(y)\rho_B(y))$, and number of AB contacts per monomer $N_{AB}/\rho(y)$ (inset), vs. y/w_{SSL} in units of $w_{SSL} = b/\sqrt{6\chi}$.

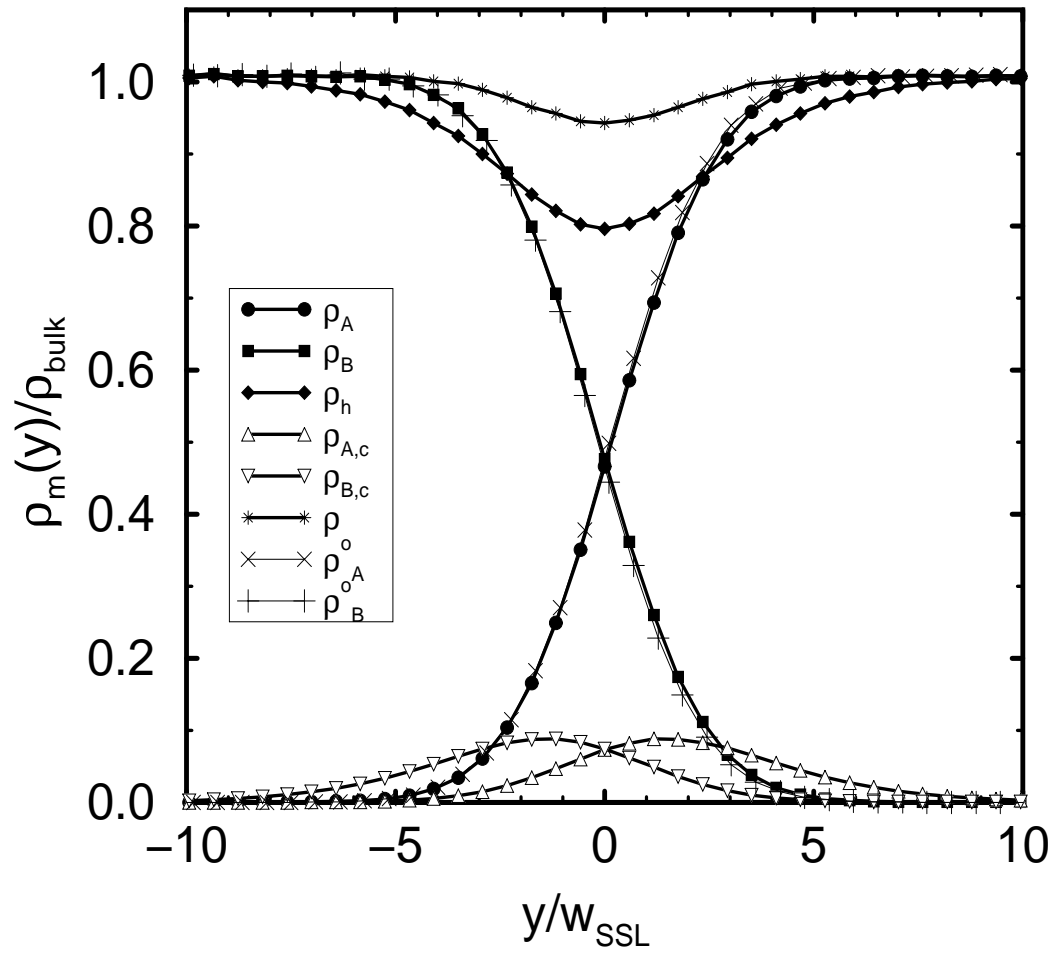


Figure 1
Werner et al

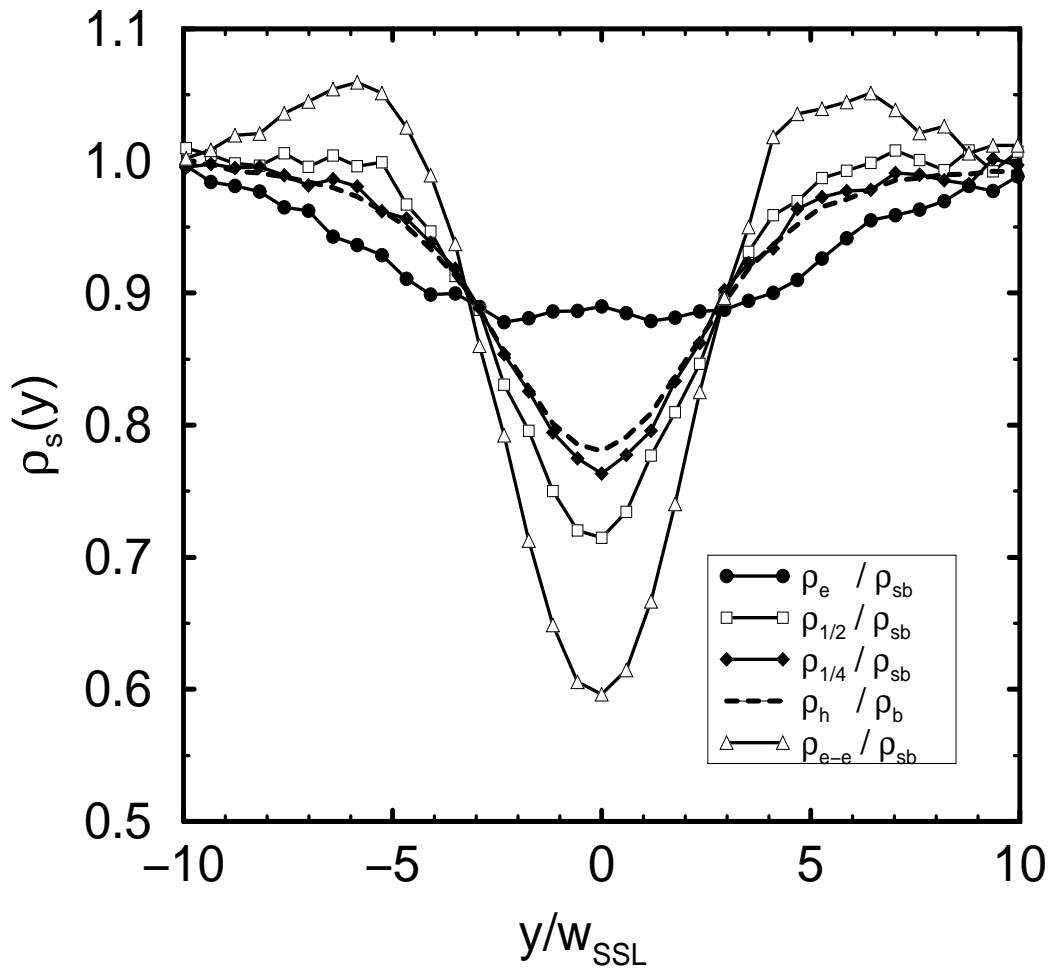


Figure 2
Werner et al

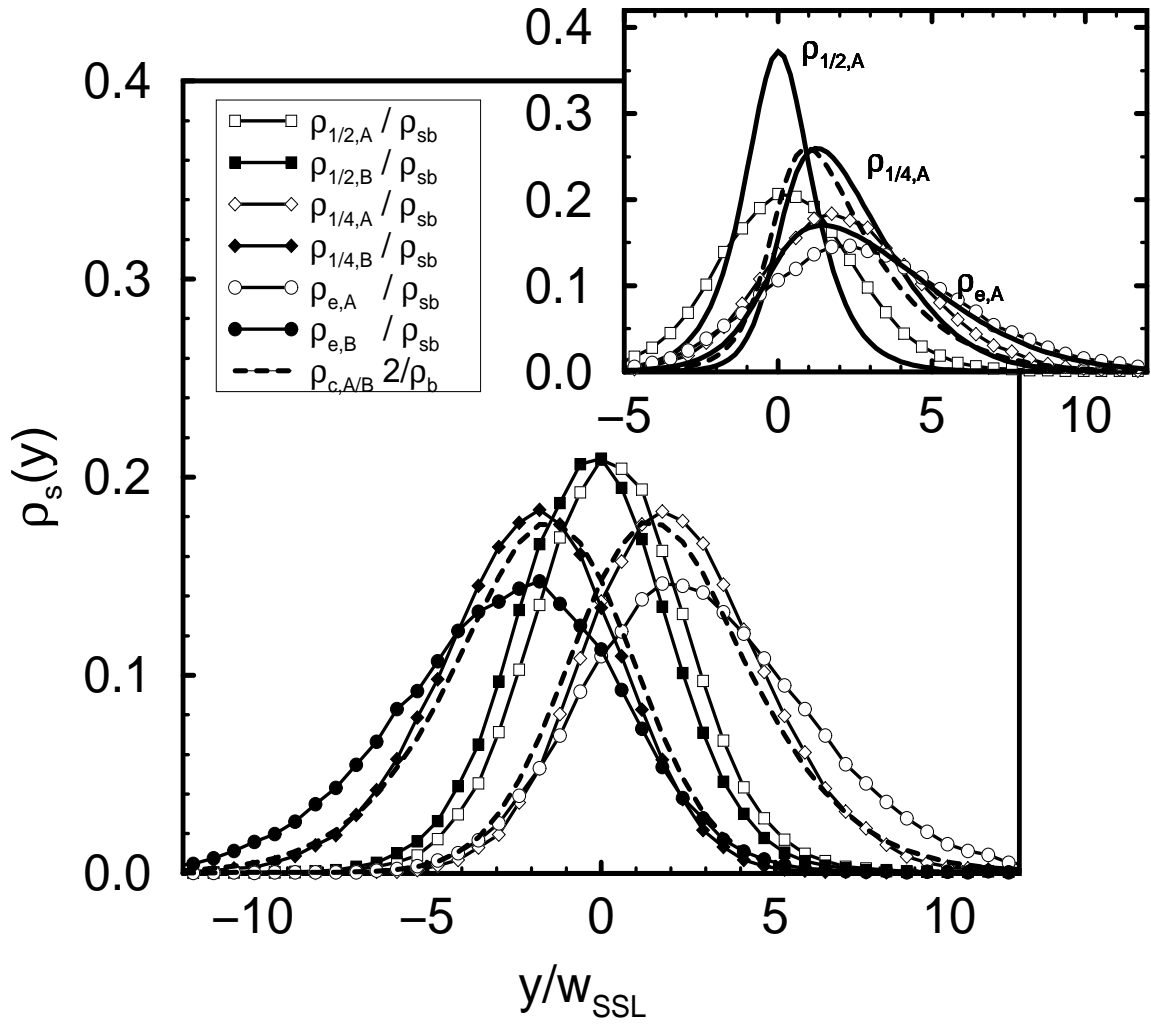


Figure 3
Werner et al

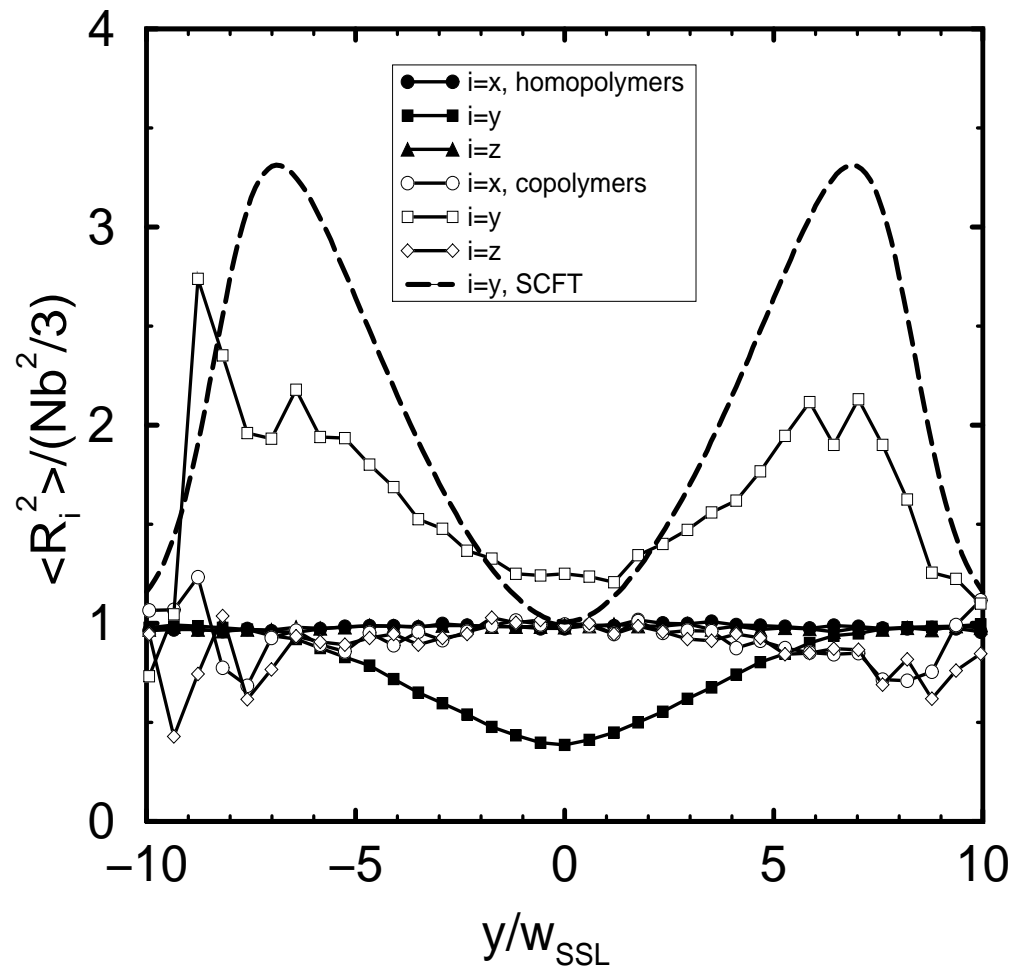


Figure 4
Werner et al

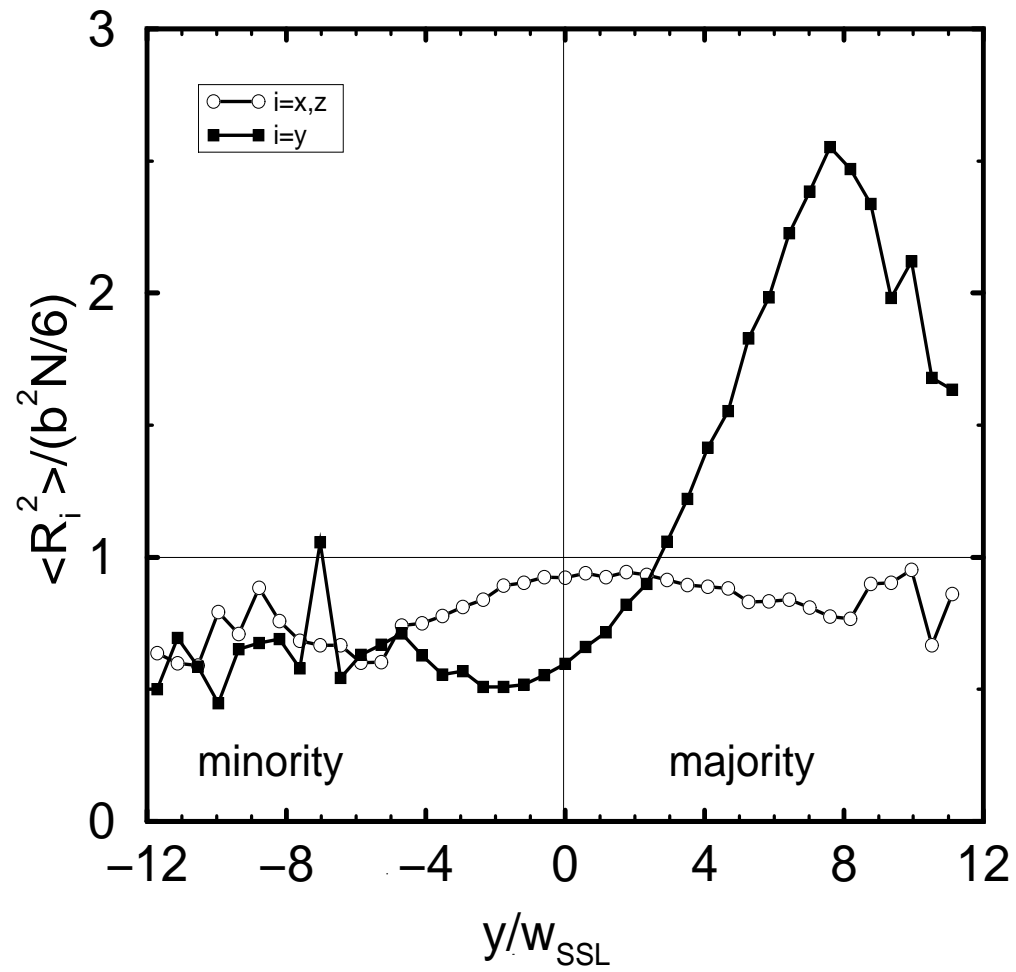


Figure 5
Werner et al

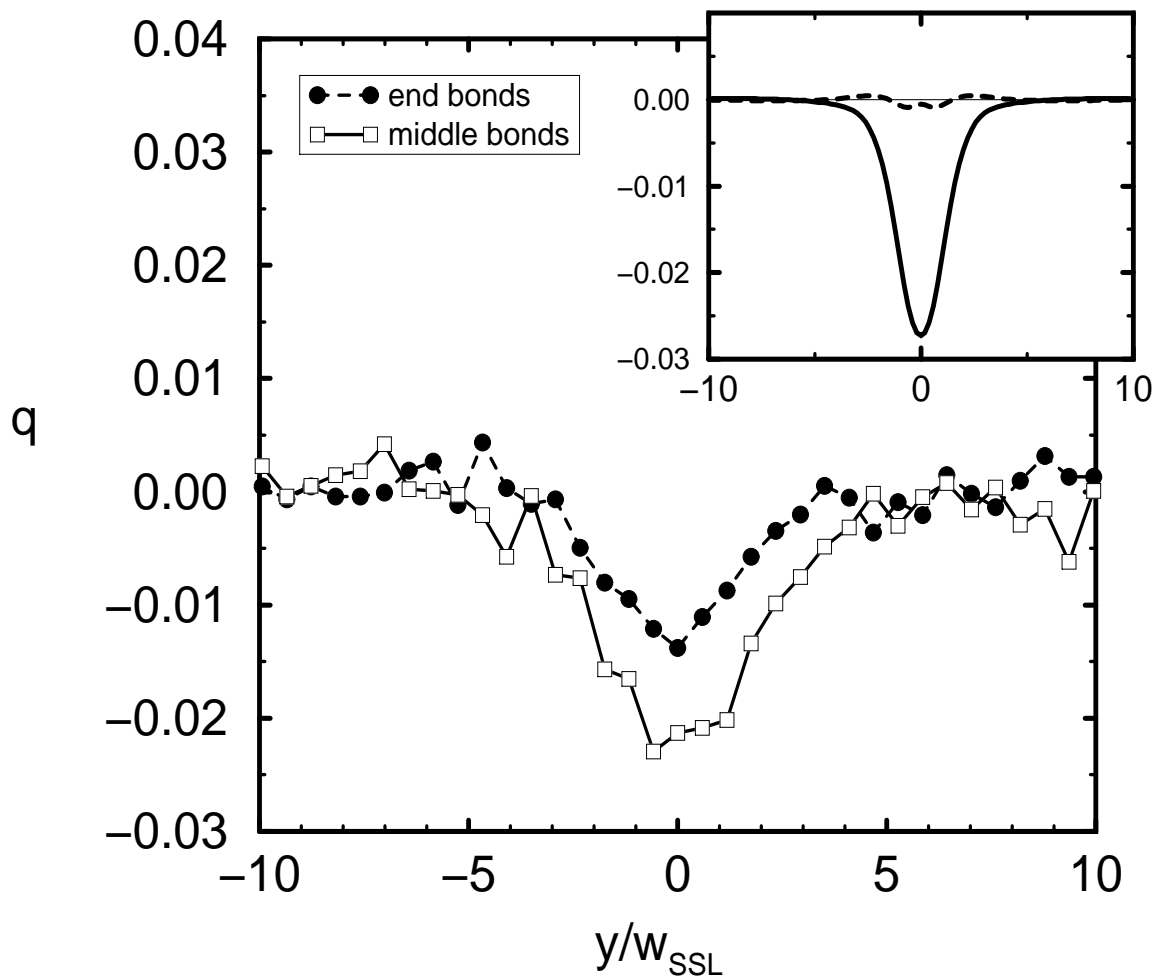


Figure 6
Werner et al

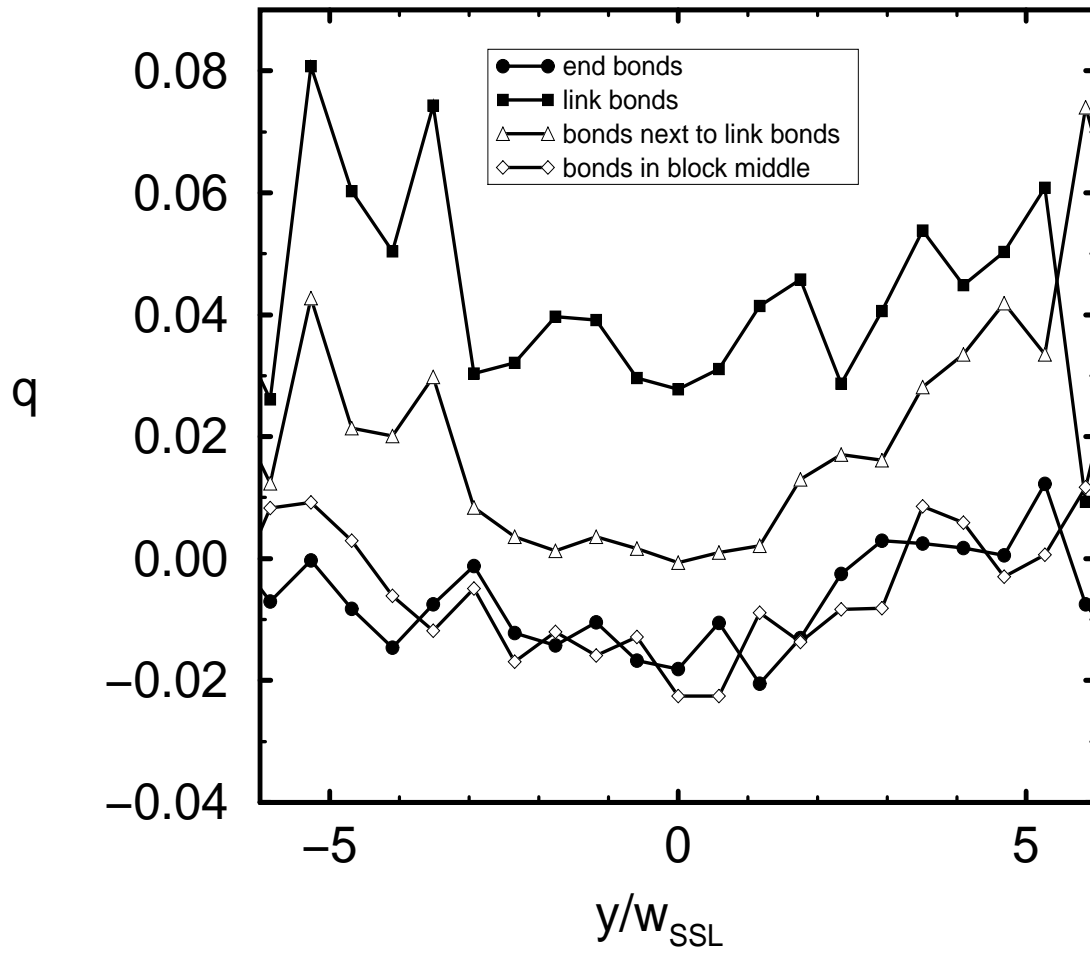


Figure 7a
Werner et al

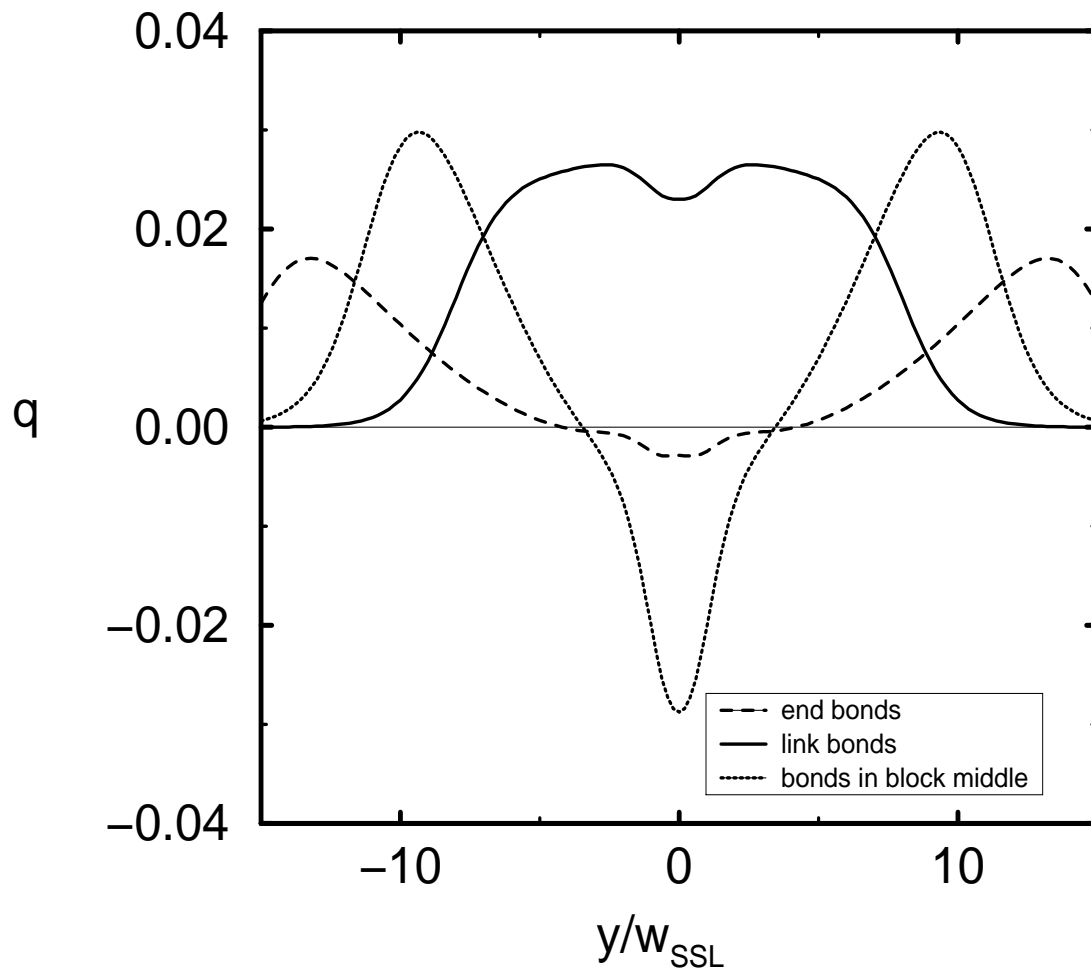


Figure 7b
Werner et al

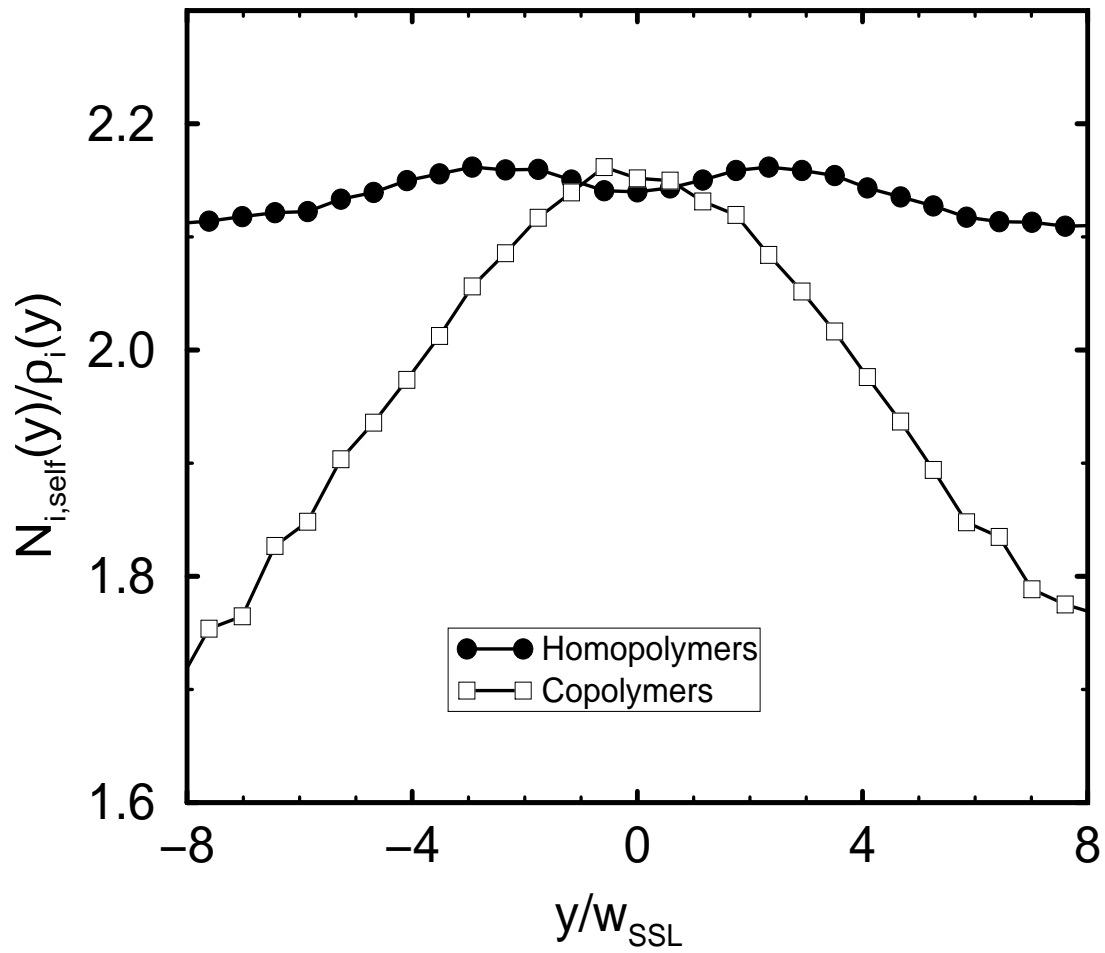


Figure 8
Werner et al

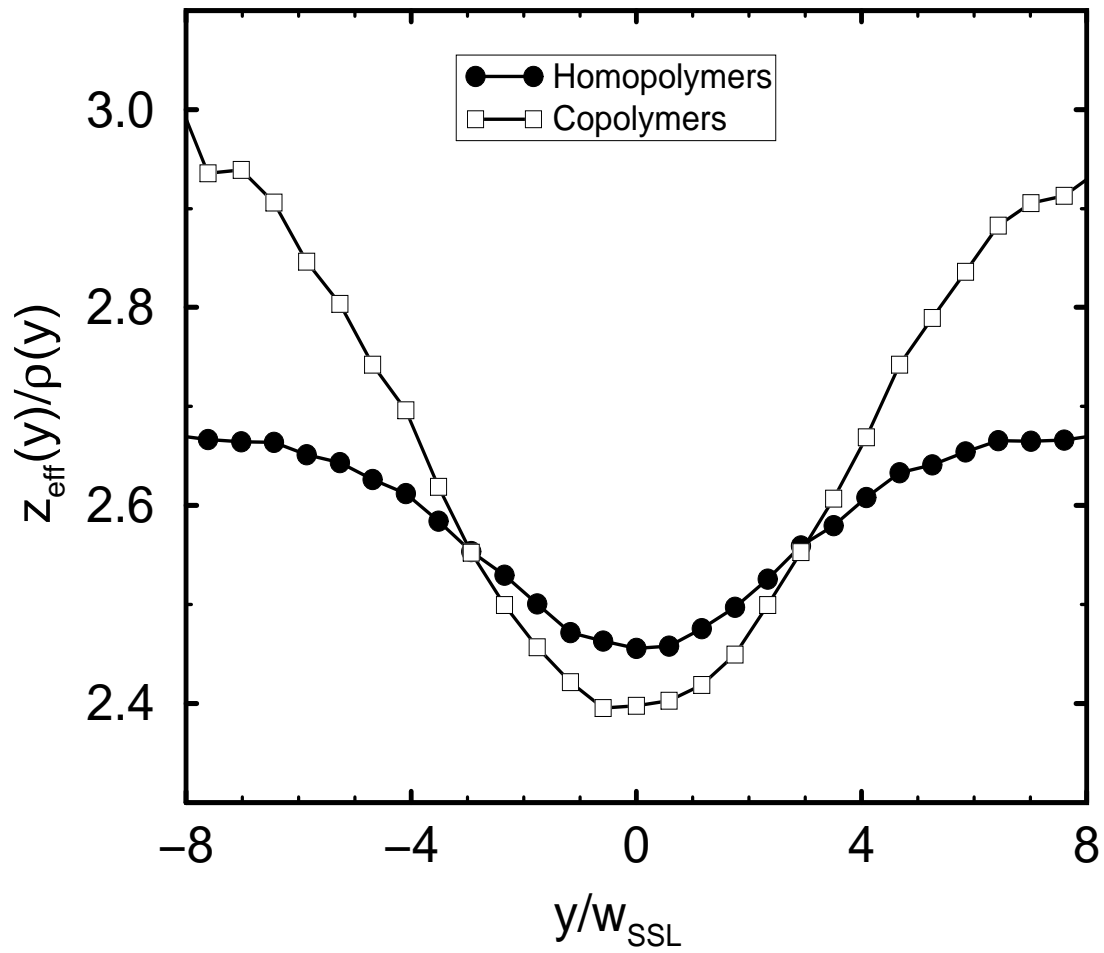


Figure 9
Werner et al

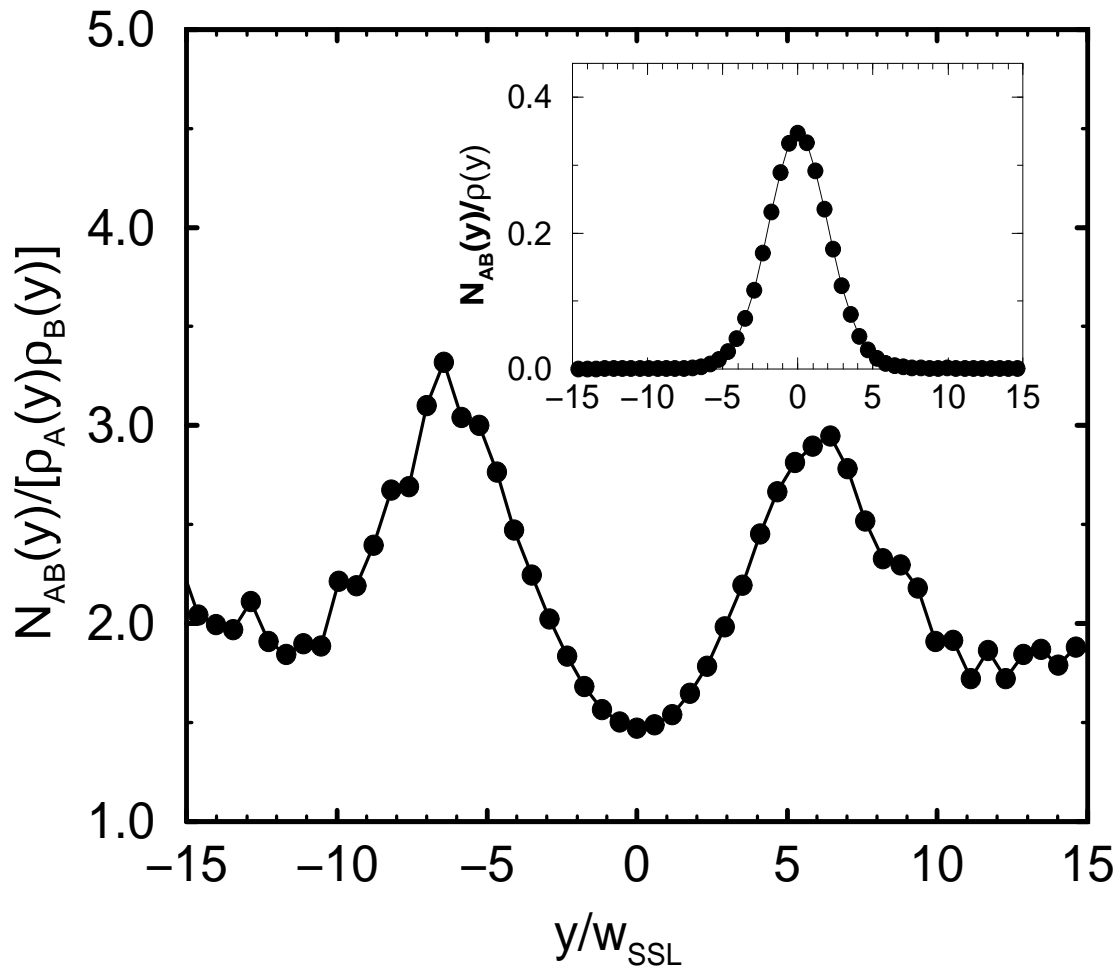


Figure 10
Werner et al

